

Polar state in epitaxial films of the relaxor ferroelectric $\text{PbMg}_{1/3}\text{Nb}_{2/3}\text{O}_3$

M. Tyunina* and J. Levoska

Microelectronics and Materials Physics Laboratories, and EMPART Research Group of Infotech Oulu, University of Oulu, PL 4500, FIN-90014 Oulun Yliopisto, Finland

K. Kundzinsh and V. Zauls

Department of Ferroelectrics and CAMART Centre of Excellence, Institute of Solid State Physics, University of Latvia, 8 Kengaraga, LV-1063 Riga, Latvia

(Received 15 November 2003; published 3 June 2004)

Dielectric response of epitaxial thin films of relaxor $\text{PbMg}_{1/3}\text{Nb}_{2/3}\text{O}_3$ was experimentally studied as a function of frequency, temperature, amplitude of ac electric field, and magnitude of dc bias. At small fields, a glass-like relaxor behavior was observed. With increasing field, an onset of a polar state was detected. Compared to bulk, such an onset was characterized by relatively low threshold fields, short critical time, and reversibility. The orientation of the polar clusters along the direction of the field and the low energy barriers between the stable states of the clusters were suggested to be responsible for the onset.

DOI: 10.1103/PhysRevB.69.224101

PACS number(s): 77.84.Dy, 77.55.+f, 77.80.-e, 77.90.+k

I. INTRODUCTION

Perovskite $\text{PbMg}_{1/3}\text{Nb}_{2/3}\text{O}_3$ (PMN) is a classic and best-studied representative of relaxor ferroelectrics (RFE). In the last decade, continuous experimental and theoretical studies of RFE have got an additional drive due to excellent electromechanical properties of RFE, which are desirable for device applications such as, e.g., microelectromechanical systems. Mechanisms of giant electrostriction effects in RFE and scaling of properties in thin-film RFE have attracted special attention.

Large strains can be observed in RFE under applied electric field. Simultaneously, both a transition from relaxor to ferroelectric (FE) state and a transition in crystal structure are possible.¹ In particular in PMN, the application of a dc electric field larger than the threshold of 0.16–0.17 MV/m results in a transition from the glass-like state to the polar FE state^{2–11} with a rhombohedral crystal structure.^{2–9} The strains obtained in RFE thin films under applied dc electric field have been found to be considerably smaller than those in single crystal RFE.^{12,13} In films, neither the electric field induced onset of the polar state, nor the transition in the crystal structure have been reported.

In the present work, to contribute to the understanding of the mechanisms governing the behavior of RFE thin films, the evolution of the state in epitaxial films of PMN under applied electric field was experimentally studied. To probe the state of the films, the dielectric response of PMN thin-film heterostructures was measured using both the bridge technique and the impedance technique combined with digital Fourier analysis.^{14,15}

According to the Landau–Ginzburg–Devonshire (LGD) approach, in FE under an ac electric field $E_{ac} = E \sin(2\pi ft)$, where E is the amplitude and f is the frequency, the amplitudes of the N th order harmonics of the relative dielectric permittivity, H_N , can be obtained in the form of polynomials of E :^{16–19}

$$H_1 \cong \varepsilon_1 + \frac{3}{4}\varepsilon_3 E^2 + \dots, \quad (1)$$

$$H_2 \cong \frac{1}{2}\varepsilon_2 E + \dots, \quad (2)$$

$$H_3 \cong \frac{1}{4}\varepsilon_3 E^2 + \dots, \quad (3)$$

where ε_1 is the linear dielectric permittivity, and ε_2 and ε_3 are the second- and third-order nonlinear dielectric permittivities, respectively. The phase angles of the odd harmonics are equal to 0° (or 180°), and those of the even harmonics are 90° . At small E in RFE with an average macroscopic cubic (or pseudocubic) crystal structure, the even harmonics are absent, i.e., $H_2 = 0$, and both ε_1 and ε_3 are functions of temperature T and frequency. A transition into a glass-like state can be identified by a peak in $\varepsilon_3(T)$ at the freezing temperature T_f , below the temperature of the dielectric maximum, T_m .^{20,21} In FE with a nonzero macroscopic polarization, all harmonics are present in the response. Also a possible contribution to the response from a Rayleigh-type motion of domain walls can result in a change of the phase angle of the third dielectric harmonic δ_3 to 90° and the appearance of the additional terms $H_1 \propto E$ and $H_3 \propto E$.¹⁸ In RFE under applied small dc electric field, H_2 is negligible and

$$H_1 \cong \varepsilon_1 + 3\varepsilon_3 E_b^2, \quad (4)$$

where E_b is the magnitude of the dc electric field. In the present work, to identify the state of the film (glass-like RFE or polar FE-like), the amplitudes H_1, H_2, H_3 and the phase δ_3 were measured and analyzed.

II. EXPERIMENT

Thin-film heterostructures consisting of a $\text{La}_{0.5}\text{Sr}_{0.5}\text{CoO}_3$ (LSCO) bottom electrode layer, a $\text{PbMg}_{1/3}\text{Nb}_{2/3}\text{O}_3$ (PMN) film with thickness of 250–270 nm, and Pt top electrodes with an area of 0.2 mm^2 were grown on MgO (001) single-crystal substrates using *in situ* pulsed laser deposition.²² A detailed x-ray diffraction analysis²³ revealed an epitaxial quality of the heterostructures. PMN films were pure perovskite, with a pseudocubic crystal structure, oriented with (001) planes parallel to the substrate (001) surface, and with

a room-temperature out-of-plane lattice parameter $a = 4.056 \text{ \AA}$. The in-plane epitaxial relationship was found to be PMN [100]||LSCO [100]||MgO[100]. The electrical characterization of the heterostructures was performed along the direction normal to the substrate surface, i.e., along [001] axes of the PMN films.

The capacitance and loss factor of the heterostructures were measured as a function of temperature $T = 100\text{--}675 \text{ K}$ and frequency $f = 10^2\text{--}10^6 \text{ Hz}$ using an HP 4284 LCR meter at the amplitude of the probing ac electric field $E = (8\text{--}10) \text{ kV/m}$, both at zero biasing field and $E_b = 7.5 \text{ MV/m}$. The real part of the small-signal dielectric permittivity $\varepsilon(f, T)$ was then determined and analyzed.

The nonlinear dielectric behavior was studied using Fourier analysis of the dielectric response of the heterostructures derived from the impedance measurements under an applied sinusoidal electric field.^{14,15} The measurements were performed at $f = 1 \text{ kHz}$ in the range of $T = 120\text{--}310 \text{ K}$.

The amplitudes of the first, second, and third dielectric harmonics (H_1, H_2, H_3), and their phases (δ_2, δ_3) were recorded in different regimes:

- as a function of temperature on cooling/heating at small ac field $E = 0.01\text{--}0.04 \text{ MV/m}$, i.e., in zero-field-cooling/heating (ZFC/H);
- as a function of the amplitude of ac field $E = 0.01\text{--}1.5 \text{ MV/m}$ at different temperatures;
- as a function of temperature on cooling/heating at small ac field and a nonzero biasing dc field E_b , i.e., in field-cooling/heating (FC/H);
- as a function of the biasing dc field E_b at small $E = 0.01 \text{ MV/m}$ and at different temperatures. In the last regime, the field E_b was swept from 0 to $\pm 20 \text{ MV/m}$ at a rate of 0.01 MV/(m s) , which could correspond to a duration of about 3–5 h for the measurement of a typical¹³ polarization–electric field loop in thin-film heterostructures. The measurement temperatures in regimes (b) and (d) were reached in ZFC from $T = 320 \text{ K}$.

The interface contribution to the dielectric response of the heterostructures was evaluated using the previously developed approach^{24,25} and assuming that the dielectric properties of the interface layers varied neither with temperature,²⁵ nor with electric field.²⁶ The true response of the films was reconstructed:

$$H_R \cong H \left(1 - \frac{\alpha_{\text{fit}} H_1}{H_{1m}} \right)^{-1}, \quad (5)$$

$$E_R \cong E \left(1 - \frac{\alpha_{\text{fit}} H_1}{H_{1m}} \right), \quad (6)$$

where indices R refer to the values reconstructed in the films, α_{fit} is a fitting parameter,²⁵ and H_{1m} is the maximum in the temperature dependence of small-signal $H_1(T)$, which is equivalent to $\varepsilon(T)$.

III. RESULTS

A. Relaxor behavior in PMN films

In PMN heterostructures, the small-signal $\varepsilon(f, T)$ measured at zero bias exhibited broad, frequency dependent maxima [Fig. 1(a)] resembling those in bulk RFE. However, in the heterostructures, both the magnitude of ε and its dependence on f could be affected by the interfaces.²⁵ Thus the state of the films (relaxor or normal ferroelectric) could be verified using the frequency dependence of the temperatures of the dielectric maxima $T_m(f)$. In PMN films, a shift of T_m to higher temperatures with increasing f was found to be relaxor-like. The relationship between the temperatures T_m and frequencies f obeyed the Vogel–Fulcher one: $\ln(f) = \ln(f_0) - T_a/(T_m - T_f)$, where f_0 , T_a , and T_f are the fitting parameters. A good linear fit to $\ln(f) \propto 1/(T_m - T_f)$ was obtained for the freezing temperature $T_f \approx 235 \text{ K}$ [Fig. 1(b)]. Although the observed T_m around 261–277 K was in agreement with that in the PMN crystals,^{27,28} the freezing temperature in the films appeared to be somewhat higher than that in the bulk (220 K).²⁸ Such a vicinity of T_f to T_m has been previously observed in the epitaxial heterostructures of various RFE and suggested to indicate a kind of ferro-glass state.²⁹

The amplitude of the first dielectric harmonic H_1 determined as a function of T at $f = 1 \text{ kHz}$ using the impedance measurements [Fig. 1(c)] coincided with the small-signal $\varepsilon(T)$ measured at $f = 1 \text{ kHz}$ using the LCR meter [Fig. 1(a)]. (This demonstrated the equivalency of the measurement techniques.) The amplitude of the third dielectric harmonic H_3 increased with decreasing temperature below T_m [Fig. 1(c)], while the amplitude of the second dielectric harmonic H_2 remained at the level of noise. The phase δ_3 was about 180° .

The amplitudes H_{1R} and H_{3R} , and the field E_R in the film were reconstructed from the data in Fig. 1(c) using Eqs. (5) and (6). The parameter $\alpha_{\text{fit}} = 0.95$ was determined from the data in Fig. 1(a). Both the linear and the third-order nonlinear dielectric permittivities, ε_1 and ε_3 , respectively, were found to depend on temperature [Fig. 1(d)]. The obtained magnitudes of ε_1 and ε_3 , the maximum in $\varepsilon_1(T)$ in the vicinity of T_m , and the maximum in $\varepsilon_3(T)$ in the vicinity of T_f were in agreement with the observations in PMN crystals.³⁰ Such a behavior [Fig. 1(d)] was consistent with the modeling^{20,21} and could evidence a glassy freezing in the film.

The results presented in Fig. 1 showed that at zero dc bias and small ac field the dielectric response of PMN films was RFE-type with indications of a glassy state.

B. Effect of ac electric field

In PMN thin-film heterostructures, with increasing amplitude of the ac electric field E , changes in $\varepsilon(f, T)$ were qualitatively similar to those typically observed in perovskite RFE.³¹ With increasing E from 0.01 to 0.4 MV/m the positions of the maxima, T_m , shifted to lower temperatures. Also

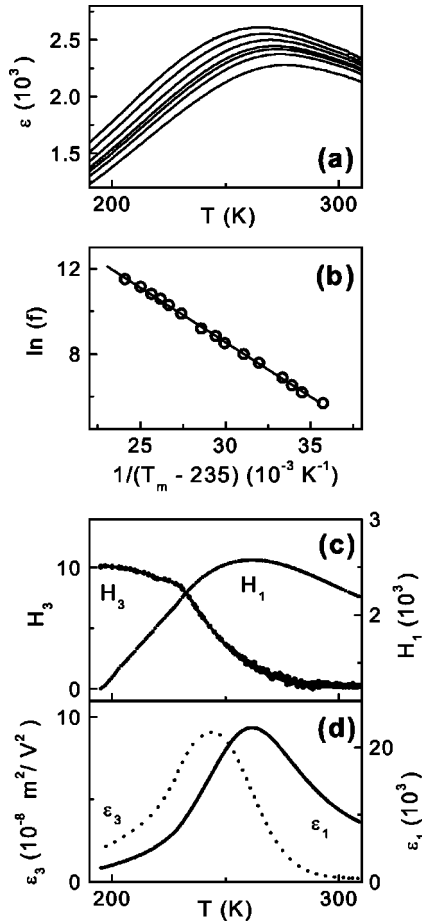


FIG. 1. Relaxor glass-like behavior of the PMN film. (a) The real part of the dielectric permittivity ε as a function of temperature T measured in the PMN thin-film heterostructure on cooling at different frequencies ($f = 1 - 100$ kHz from the upper curve down) and small ac field $E = 10$ kV/m. (b) The relationship between the measurement frequency f and the temperature of the dielectric maximum T_m in PMN film. Straight line shows fit to the Vogel-Fulcher relationship. (c) The amplitudes of the first and third dielectric harmonics, H_1 and H_3 , as a function of temperature measured in PMN thin-film heterostructure on cooling at $f = 1$ kHz and $E = 10$ kV/m. (d) The linear and the third-order nonlinear dielectric permittivities, ε_1 (shown by line) and ε_3 (shown by dashed line), as a function of temperature. Both ε_1 and ε_3 are reconstructed in the PMN film using the amplitudes H_1 and H_3 measured in the heterostructure.

an increase in the permittivity ε around T_m could be detected, although it was suppressed due to the interface contribution.³²

Studies of the nonlinear dielectric response around and below T_m showed that in the heterostructures, with increasing E from 0.01 to about 0.5 MV/m the amplitudes of the first and third harmonics, H_1 and H_3 , increased, and the amplitude of the second harmonic H_2 did not exceed the noise level. The true response of the films was evaluated as described earlier, and the field dependencies of the reconstructed amplitudes H_{1R} and H_{3R} were analyzed. Good linear fits to $H_{1R} \propto E_R^2$ and $H_{3R} \propto E_R^2$ were obtained for $E_R = 0 - 0.02$ MV/m [Fig. 2(a)], in agreement with Eqs. (1) and (3). The third-order nonlinear dielectric permittivity ε_3 de-

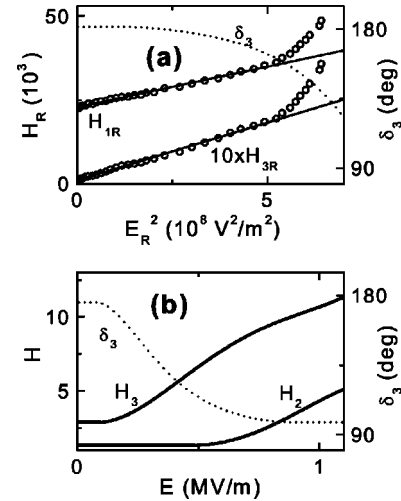


FIG. 2. Effect of ac electric field. (a) The amplitudes of the first and third dielectric harmonics reconstructed in the PMN film, H_{1R} and H_{3R} (both are shown by open circles), and the phase angle of the third dielectric harmonic δ_3 (shown by dashed line) as a function of the square of the amplitude of the ac field seen by the film, E_R^2 , determined at $f = 1$ kHz and $T = 253$ K. Straight lines are fits to $H_{1R} \propto E_R^2$ and $H_{3R} \propto E_R^2$. (b) The amplitudes of the second and third dielectric harmonics, H_2 and H_3 (lines are averaged and smoothed data), and the phase angle of the third dielectric harmonic δ_3 (dashed line) as a function of amplitude of the applied ac electric field E measured in the PMN thin-film heterostructure at $f = 1$ kHz and $T = 265$ K.

termined from the slope of the linear fit $H_{1R} \propto E_R^2$ coincided with that determined from the slope of $H_{3R} \propto E_R^2$ and with that in Fig. 1(d).

With increasing E_R above 0.02 MV/m, a deviation from the square field dependence of both H_{1R} and H_{3R} was found. In relaxor ceramic 9/65/35 PLZT and PMN single crystals, an additional third-order contribution ($\propto E^3$) with a negative sign has been found in the ac field dependence of the first harmonic H_1 .³³ This has been modeled as a result of the possible displacement of polar clusters from their equilibrium positions by the applied electric field and, respectively, a field modulation of the intercluster coupling.²¹ In contrast to such an expected behavior of the amplitude H_{1R} , the observed increase in both the amplitude of H_{1R} and H_{3R} at $E_R > 0.02$ MV/m could be connected with the linear contribution ($\propto E$) due to the possible motion of the phase boundary (e.g., nano-domain wall motion).¹⁸ Such a possibility was in agreement with the phase angle of the third harmonic δ_3 , which began “switching” from about 180° toward 90° [dashed line in Fig. 2(a)].

The observed change of the response [Fig. 2(a)] showed that the “pure” glass-like RFE state of the film was disturbed. However, an onset of a polar state, which could be evidenced by an increase of the amplitude of the second harmonic H_2 , was detected at larger fields. [For example, in Fig. 2(b), with increasing amplitude E the phase δ_3 began changing at about $E = 0.15$ MV/m ($E_R = 0.02$ MV/m), while the amplitude H_2 began increasing at $E > 0.5$ MV/m ($E_R > 0.08$ MV/m)]. The amplitude H_2 remained smaller than

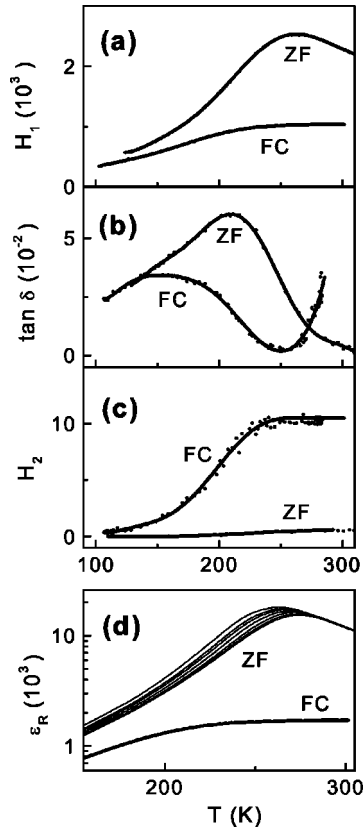


FIG. 3. Effect of dc electric field. The amplitude of the first dielectric harmonic H_1 (a), loss factor $\tan \delta$ (b), the amplitude of the second dielectric harmonic H_2 (c), and the reconstructed dielectric permittivity ϵ_R (d) as a function of temperature determined in the PMN thin-film heterostructure at zero dc field $E_b = 0$ (lines marked with ZF) and nonzero dc field $E_b = 7.5$ MV/m (lines marked with FC). The lines are averaged and smoothed data. Frequency f is (a), (b), (c) $f = 1$ kHz and (d) $f = 1-50$ kHz from the upper curves down.

H_3 even at large $E > 1$ MV/m, in contrast to the response of films in normal FE state with $H_1 > H_2 > H_3$.¹⁴

The results presented in Fig. 2 showed that in PMN films, with increasing amplitude of the ac electric field the glass-like RFE state was disturbed (at $E_R \geq 0.02$ MV/m) and a polar state was induced (at $E_R \geq 0.08$ MV/m). The threshold fields E_R in the range of 0.02–0.08 MV/m were in general agreement with the field $E = 0.04$ MV/m, at which the glassy freezing in single-crystal PMN has been found to be destroyed.²⁸

C. Effect of dc electric field

In PMN thin-film heterostructures, both ZFC and ZFH experiments revealed no difference in the responses obtained on cooling and heating runs. Compared to ZFC, cooling under applied dc electric field (FC) resulted in a decrease of the amplitude H_1 in the whole range of $T = 100-310$ K [Fig. 3(a)], a decrease of $\tan \delta$ with a shift of maximum toward lower T [Fig. 3(b)], and a considerable increase of the amplitude of the second harmonic H_2 [Fig. 3(c)]. Also only a minor, interface related,²³⁻²⁵ frequency dispersion of permit-

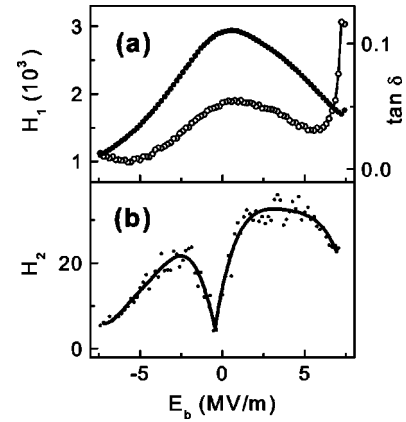


FIG. 4. (a) The amplitude of the first dielectric harmonic H_1 and loss factor $\tan \delta$, and (b) the amplitude of the second dielectric harmonic H_2 (line shows averaged and smoothed data) as a function of applied dc electric field E_b measured in the PMN thin-film heterostructure at $T = 261$ K.

tivity $\epsilon(f)$ was observed in the whole temperature range. No frequency dependence of T_m was detected. The changes were more clearly seen in the behavior of the reconstructed permittivity $\epsilon_R(f, T)$ [Fig. 3(d)]. Response in the field-heating run (FH) after ZFC run resembled qualitatively the FC response.

In accordance with the observations in bulk RFE,²⁻¹¹ the results in Fig. 3 showed an onset of a polar ferroelectric-like phase under applied dc electric field. However, neither an expected⁶ sequence of transformations with corresponding changes in $H_1(T)$ or $\epsilon(T)$, nor a difference between FC and FH runs, nor a peak in H_1 around 215 K were observed. In part, this could be ascribed to the influence of the interface layers and a suppression of the amplitudes H_1 , H_2 , and ϵ . For example, a possible presence of two dielectric maxima or difference between T_m in FC and FH could become hardly detectable for such a smeared maximum in $H_1(T)$ as that for FC in Fig. 3(a). However, a peculiar nature of the polar phase in thin films should be considered, too.

The stability of the induced polar phase was probed by switching the dc electric field on and off during the cooling and/or heating. A complete reversibility of the responses was observed, i.e., with the field on, the response corresponded to the FC curves in Fig. 3, while without the field it coincided with the ZFC curves in Fig. 3. Such a reversibility was in contrast to the FC regime in PMN crystals, where the polar phase has been found to be stable without field to $T = 208$ K.⁴

The observed instability of the polar phase allowed its study by varying E_b at a sweeping rate of 0.01 MV/(m s). In PMN heterostructures at a fixed temperature with increasing magnitude of E_b , the amplitude of the first harmonic H_1 and loss factor $\tan \delta$ were found to decrease [Fig. 4(a)], and the amplitude of the second harmonic H_2 first strongly increased and then decreased [Fig. 4(b)]. The repeated cycling of the field E_b did not result in a detectable change of the response.

The response was asymmetric with respect to the polarity of the dc field. Similar asymmetry [Fig. 4(a)] has been often observed in ferroelectric thin-film heterostructures and as-

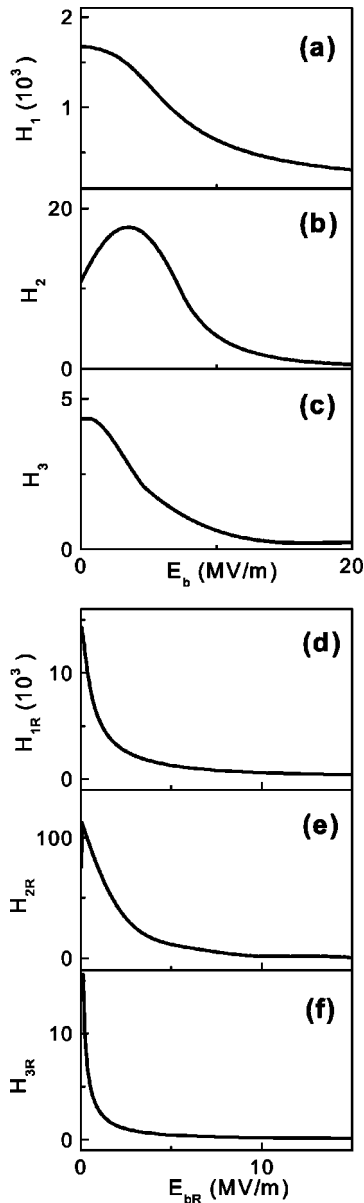


FIG. 5. The amplitudes of the (a) first H_1 , (b) second H_2 , and (c) third H_3 dielectric harmonics as a function of the magnitude of the applied dc electric field E_b measured in the PMN thin-film heterostructure at $T=247$ K. The reconstructed amplitudes of the (d) first H_{1R} , (e) second H_{2R} , and (f) third H_{3R} dielectric harmonics in the PMN film as a function of the field E_{bR} seen by the film, determined at $T=247$ K. The data are averaged and smoothed.

cribed to the difference between top and bottom electrode layers, with possible carrier injection influenced by a space charge at the Pt interface.³⁴ (This could determine an increase in $\tan \delta$ at $E_b = +7$ MV/m.) Further on, only the branches of the response with a monotonic decrease in $\tan \delta$ ($E_b < 0$ in Fig. 4) were taken into consideration.

For different temperatures, a typical monotonic branch of the response of the PMN heterostructure was qualitatively the same as that presented in Fig. 5. Unfortunately, small magnitudes of H_1 and H_2 at low temperatures limited the range of the studied temperatures to 170–300 K. Also the

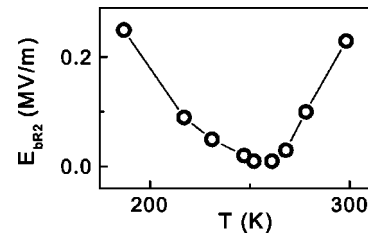


FIG. 6. The critical field E_{bR2} necessary for the onset of the polar phase in the PMN film as a function of temperature.

amplitude of the third harmonic $H_3(E_b)$ could be reliably detected only in the range of $T=200$ – 265 K. In the whole studied range of temperatures, the relationship $H_1 > H_2 > H_3$ was characteristic for the polar phase.

The true response of the film was reconstructed using Eqs. (5) and (6) [Figs. 5(d) and 5(e)]. With increasing field E_{bR} seen by the film, an initial increase of the reconstructed amplitude H_{2R} appeared to be very steep, so that the critical field E_{bR2} necessary for the onset of the polar phase was determined as that corresponding to the maximum H_{2R} . For the temperatures $200 \text{ K} < T < 300 \text{ K}$, the field E_{bR2} (Fig. 6) was smaller than the threshold field of 0.16–0.17 MV/m in PMN crystals. Such a discrepancy might be related to the reconstruction procedure. However, the obtained agreement of the amplitudes H_{1R} , ε_1 , ε_3 , and threshold ac field E_R reconstructed in the films with the corresponding values in the PMN crystals pointed to a minor uncertainty of the reconstruction.

In PMN crystals, the critical time τ necessary for the onset of the ferroelectric behavior has been found to depend on both the magnitude of the field and temperature.^{4,9} For example, extrapolation of the data from Ref. 9 showed that for $T < 200$ K with increasing field from 0.2 to 1.5 MV/m, the time τ decreased from 10^5 – 10^6 s to 10^{-1} s. Considering the crystal τ – T diagram and assuming that in the heterostructures in the sweeping regime the polar phase was formed during a few seconds, the field E_{bR2} should monotonically increase from about 0.25 to 1.5 MV/m with decreasing T from that around T_m to 170 K. Qualitatively, an increase of E_{bR2} with decreasing T below T_m in Fig. 5(g) was consistent with such expectations. Also for the temperatures above T_m , larger fields E_{bR2} were in a qualitative agreement with the phase diagram of crystal PMN.

Nevertheless, the observed small critical fields E_{bR2} , supposed short critical times, instability of the polar phase, similarity of the changes both below and above T_m , indicated a peculiarity of the crossover from nonequilibrium dipole glass state to the polar state in the films compared to that in the crystal PMN. To get a better insight in it, both the behavior of polarization and amplitudes $H_R(E_{bR})$ were analyzed in detail.

D. Polar phase

In PMN thin-film heterostructures, the polar phase might be compared to a homogeneous, polarized ferroelectric.

In the PMN heterostructures, polarization P was determined by integrating the dependencies $H_1(E_b)$ at different

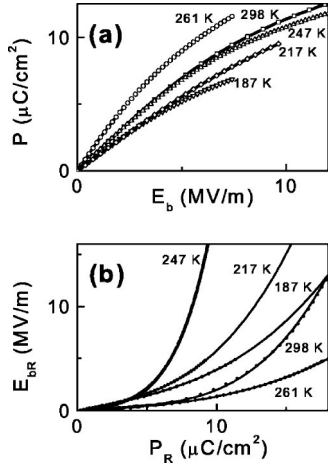


FIG. 7. (a) Polarization P as a function of the field E_b determined in the PMN thin-film heterostructure at different temperatures. (b) The relationship between the reconstructed polarization P_R in the PMN film and the field E_{bR} seen by the film determined at different temperatures. The lines are fits to $E_{bR} \approx a_1(P_R - P_0) + a_2(P_R - P_0)^2 + a_3(P_R - P_0)^3$.

temperatures. The obtained $P(E_b)$ curves [Fig. 7(a)] resembled those observed in ferroelectric thin-film heterostructures.²⁶ In the PMN films, the reconstructed field E_{bR} was analyzed as a function of the reconstructed polarization P_R , which was determined by integrating the dependencies $H_{1R}(E_{bR})$. The relationship between E_{bR} and P_R [Fig. 7(b)] appeared to satisfy

$$E_{bR} \approx a_1(P_R - P_0) + a_2(P_R - P_0)^2 + a_3(P_R - P_0)^3, \quad (7)$$

$$P_R > P_0 > 0,$$

where the fitting parameters were $a_1 \approx (0.7-2.7) \times 10^7$ V m/C, $a_2 = -(5-40) \times 10^{10}$ V m³/C², $a_3 \approx (5-35) \times 10^{17}$ V m⁵/C³, and the polarization $P_0 \approx 0.1-0.3$ μ C/cm². The form of Eq. (7) was in agreement with the equation of state obtained recently³⁵ rather than with that in the LGD model.

In the PMN thin-film heterostructures with increasing field E_b , the amplitude H_1 decreased. According to the LGD model in perovskite paraelectrics, relaxors, and ferroelectrics, the field dependence of the amplitude H_1 can be generally expressed as a polynomial of field. Thus, for the polar phase of the PMN film, a polynomial fit to $H_{1R}(E_{bR})$ would be expected, too. However, neither the measured dependence $H_1(E_b)$ nor the reconstructed one, $H_{1R}(E_{bR})$, could be satisfactorily described by any high-order (to the eighth order) polynomials. In a broad range of large E_b , the field dependence of the amplitude H_1 could be described by the relationship $1/H_1 \propto E_b$ [the linear fit to $1/H_1 \propto E_b$ in Fig. 8(a)]. For the reconstructed amplitude H_{1R} , a good linear fit to the dependence of $1/H_{1R}$ on E_{bR} was obtained for $E_{bR} > 0.5$ MV/m [Fig. 8(b)].

The linear relationship between $1/H_{1R}$ and E_{bR} was found in the whole studied range of temperatures [Figs. 9(a)–9(c)].

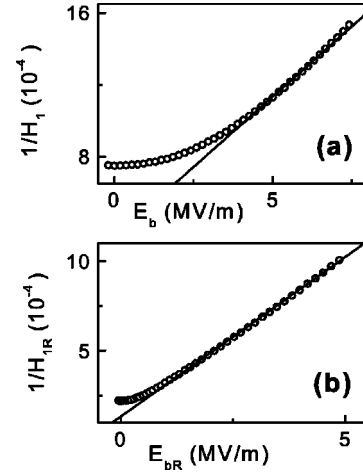


FIG. 8. The inverse amplitude of the first dielectric harmonic $1/H_1$ as a function of the field E_b determined in the PMN thin-film heterostructure at $T=217$ K. Straight line shows fit to $1/H_1 \propto E_b$. (b) The inverse reconstructed amplitude of the first dielectric harmonic $1/H_{1R}$ in the PMN film as a function of the field E_{bR} seen by the film determined at $T=217$ K. Straight line shows fit to $1/H_{1R} \propto E_{bR}$.

Thus at fields $|E_{bR}| > 0.5-1.0$ MV/m, the field dependence of the amplitude of the first dielectric harmonic could be approximately described by

$$H_{1R} \approx \frac{1}{A_1 + B_1|E_{bR}|}, \quad (8)$$

where the parameters A_1 and B_1 could be found from the linear fits to $1/H_{1R} \propto E_{bR}$.

Also for the field dependence of the amplitude H_3 of the third dielectric harmonic, both the observed behavior of $H_3(E_b)$ and the reconstructed behavior of $H_{3R}(E_{bR})$ were of similar character to those of the amplitude of the first dielectric harmonic $H_1(E_b)$ and $H_{1R}(E_{bR})$, respectively. The expected polynomial field dependence was not detected. Rather the relationship $1/H_{3R} \propto E_{bR}$ was valid [Figs. 9(d) and 9(e)]. Similar to Eq. (8), an Expression (9) for the field dependence of the amplitude of the third harmonic could be written in form

$$H_{3R} \approx \frac{1}{A_3 + B_3|E_{bR}|}, \quad (9)$$

where the parameters A_3 and B_3 could be found from the linear fits to $1/H_{3R} \propto E_{bR}$.

All parameters A_1 , A_3 , B_1 , and B_3 were functions of temperature [Figs. 10(a) and 10(b)]. The temperature evolution of A_3 and B_3 was in qualitative agreement with that of A_1 and B_1 , respectively.

A deviation from Eq. (8) was clearly seen in the behavior of $H_{1R}(E_{bR})$ at smaller fields $E_{bR} < 0.5$ MV/m [Figs. 11(a) and 11(b)]. Such a bell-shaped decay [better seen in Fig. 11(a)] resembled the dc field dependence of permittivity observed previously in KTaO_3 ,³⁶ $\text{Sr}_{1-x}\text{Ca}_x\text{TiO}_3$,³⁷ and $\text{Cd}_2\text{Nb}_2\text{O}_7$.³⁸ The decay has been ascribed to the polarization contribution originating from the reorientation of polar

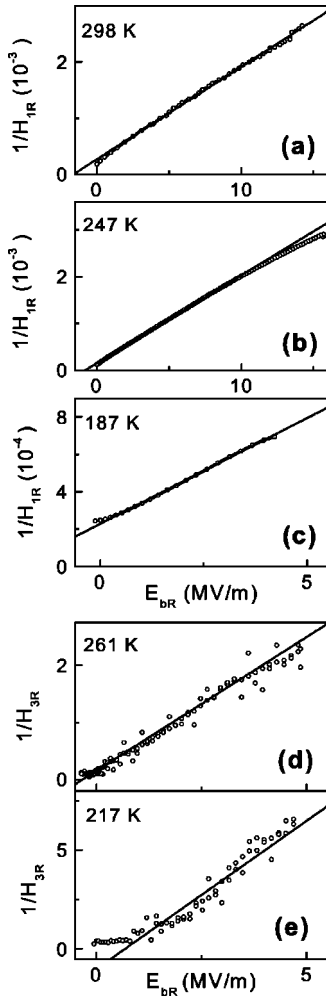


FIG. 9. The inverse reconstructed amplitude of the first dielectric harmonic $1/H_{1R}$ as a function of the field E_{bR} determined in the PMN film at (a) $T=298$ K, (b) $T=247$ K, and (c) $T=187$ K, and the inverse reconstructed amplitude of the third dielectric harmonic $1/H_{3R}$ as a function of the field E_{bR} determined in the PMN film at (d) $T=261$ K and (e) $T=217$ K. The straight lines show the fits to $1/H_{1R} \propto E_{bR}$ and $1/H_{3R} \propto E_{bR}$.

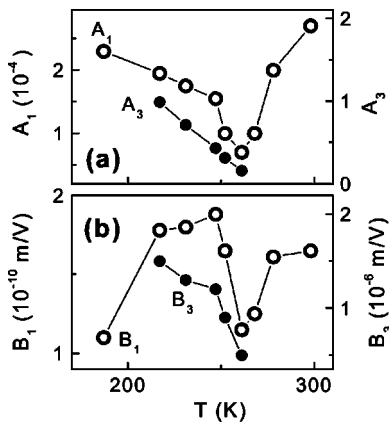


FIG. 10. The fitting parameters (a) A_1 and A_3 , and the parameters (b) B_1 and B_3 as a function of temperature determined in the PMN film from the linear fits to $1/H_{1R} \propto E_{bR}$ and $1/H_{3R} \propto E_{bR}$ at $E_{bR} > 0.5$ MV/m.

clusters. To evaluate the possibility of such a contribution to the dielectric response of PMN films, the small-field $H_{1R}(E_{bR})$ was analyzed using a modified Langevin-type approach.^{39,40}

In the pseudocubic perovskite [001] oriented film containing n_p polar regions with the dipole moments p and concentration $N = n_p/V$, the polarization P , which results from the clusters orientation and is parallel to the small electric field E applied along [001] crystal direction, could be given by

$$P = Np \tanh\left(\frac{pE}{kT}\right) + \epsilon_0 \epsilon_\infty E, \quad (10)$$

where k is the Boltzmann constant, ϵ_0 is the dielectric permittivity of the vacuum, and ϵ_∞ characterizes the pure response of the crystal lattice. Respectively, the corresponding real part of the dielectric permittivity ϵ_p can be presented as

$$\epsilon_p = \frac{kTN}{\epsilon_0} z^2 [\cosh(zE)]^{-2} + \epsilon_\infty, \quad (11)$$

where $z = p/kT$. It should be noted that Eqs. (10) and (11) differ from those used in the previous works,^{36–39} where the clusters were supposed to occupy the whole volume of the sample.

Good fits of the dependencies $H_{1R}(E_{bR})$ at small fields $0 < E_{bR} < (0.5–1.0)$ MV/m to Eq. (11) with a temperature-dependent ϵ_∞ ⁴⁰ were obtained [Figs. 11(a) and 11(b)] in the whole studied range of temperatures. The dipole moment $p \approx (1–15) \times 10^{-27}$ C m and the concentration $N \approx (0.4–10) \times 10^{25}$ m⁻³ [Figs. 11(c) and 11(d)] determined from the best fits were found to be of the same order of magnitude as those in PMN ceramics.⁴⁰ The size L of the polar clusters was estimated using the obtained dipole moment p and assuming the effective charge and ionic displacements typical for the perovskite $\text{PbB}^1\text{B}^{II}\text{O}_3$ relaxors.⁴¹ It was in the range of $L = 10–30$ Å, also in agreement with that found in PMN ceramics.⁴⁰ [The polar clusters of such a size and density as in Fig. 11(d) could occupy about 10% of the volume of the film.]

At small electric fields such that $z \cdot E < 1$, Eq. (11) could be approximated by

$$\epsilon_p \cong \frac{kTN}{\epsilon_0} \left(z^2 - z^4 E^2 + \frac{2}{3} z^6 E^4 + \dots \right). \quad (12)$$

This allowed the evaluation of the small-signal dc field related linear permittivity $\epsilon_1^{(dc)}$ and third-order nonlinear permittivity $\epsilon_3^{(dc)}$ using the obtained p and N , and considering Eq. (4):

$$\epsilon_1^{(dc)} \cong \frac{Np^2}{\epsilon_0 kT}, \quad (13)$$

$$\epsilon_3^{(dc)} \cong -\frac{Np^4}{3\epsilon_0 (kT)^3}. \quad (14)$$

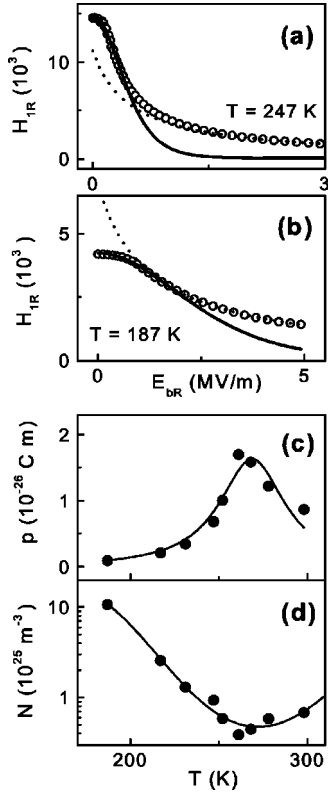


FIG. 11. The reconstructed amplitude of the first dielectric harmonic H_{1R} in the PMN film as a function of the field E_{bR} seen by the film at (a) $T=247$ K and $T=187$ K. Open circles show H_{1R} , dashed lines are fits to Eq. (8), and thick lines are fits to Eq. (11). The dipole moment p (c) and concentration N (d) of the polar clusters as a function of temperature. The lines are guides for eye.

The temperature evolution of thus calculated $\varepsilon_1^{(dc)}$ and $\varepsilon_3^{(dc)}$ is presented in Fig. 12. A satisfactory agreement was obtained between the linear permittivity $\varepsilon_1^{(dc)}$ extracted from the measurements with sweeping the dc field and that ε_1 obtained in ZFC [Fig. 12(a)]. The dc field related $\varepsilon_3^{(dc)}$ had opposite sign to that of ε_3 obtained in ZFC, in qualitative agreement with the behavior in a PMN $\langle 100 \rangle$ crystal,⁴² although the magnitude of $\varepsilon_3^{(dc)}$ appeared to be somewhat larger [Fig. 12(b)]. Also similar to the behavior in a PMN $\langle 100 \rangle$ crystal,⁴² the temperature of the maximum magnitude of $\varepsilon_3^{(dc)}$ was shifted to higher T with respect to that of maximum ε_3 . Despite the similarities of $\varepsilon_3^{(dc)}$ in the film with that in the crystal,⁴² the obtained $\varepsilon_3^{(dc)}$ did not correspond to the pure relaxor state, but rather to a polar phase as it was evidenced here (Fig. 3). This was in contrast to Ref. 42, where the relaxor state was considered to be undisturbed.

In the analysis of the amplitude $H_{1R}(E_{bR})$ at small E_{bR} , Eqs. (10) and (11) for the static response were applied to the dynamic response which is not equivalent to the static one. Neither the volume fraction, nor distributions of the orienting clusters were taken into account. Despite such assumptions, the obtained results [Figs. 11(c), 11(d), 12(a), and 12(b)] were both self-consistent and consistent with the previous observations. They showed that in PMN films, the field-induced reorientation of polar clusters could be responsible

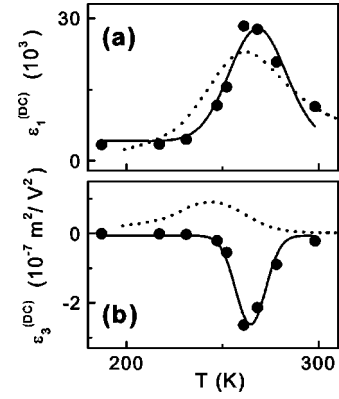


FIG. 12. (a) The linear and (b) third-order nonlinear dielectric permittivities, $\varepsilon_1^{(dc)}$ and $\varepsilon_3^{(dc)}$, determined in the PMN film at small dc electric fields as a function of temperature (circles). The lines are guides for eye. The dashed lines show the linear and third-order nonlinear dielectric permittivities, ε_1 and ε_3 , obtained in the PMN film at zero dc field.

for the onset of the polar phase at the relatively small threshold fields (Fig. 6). Such mechanism seemed to be dominating at the fields below 0.5–1.0 MV/m. At larger dc fields the response was, probably, determined by another mechanism, which could be presented by Eq. (8).

Equation (8) describes a linear field dependence of the inverse permittivity at large enough fields. It has been shown recently³⁵ that in a system of Langevin microdipoles with constant $\langle |\mathbf{p}|^2 \rangle$, fluctuations of the direction of the dipole moment are possible. In the relatively strong fields E , this leads to $\varepsilon \propto E^{-1/2}$. Although Eq. (8) did not correspond exactly to the expected relationship $\varepsilon \propto E^{-1/2}$, the obtained dependence $H_{1R} \propto E_{bR}^{-1}$ could indicate a contribution from fluctuation polarization.

IV. DISCUSSION

In epitaxial PMN thin films at zero dc field and small amplitudes of ac probing field, a typical relaxor behavior with indications of glassy freezing was observed. A crossover from nonequilibrium dipole glass state to the polar state was induced by applying dc electric field. The threshold fields for such an onset of the polar phase appeared to be small compared to that of 0.17 MV/m in PMN crystals. The estimated critical time for the onset was short: less than 1–2 s. The polar phase was unstable in the temperature range of $T=130$ –310 K. The dielectric response was completely reversible between the regimes (ZFC, ZFH, FC, or FH) at fields to 20 MV/m. At fields smaller than 0.5–1.0 MV/m, the dielectric permittivity could be satisfactorily described as that originating from the reorientation of the polar clusters. At fields larger than 0.5–1.0 MV/m, a linear field dependence of the inverse permittivity was found. With increasing dc field or with increasing duration of the measurements, dielectric anomalies, which would indicate structural transitions, were not detected.

These experimental observations revealed a peculiar nature of the polar phase in the epitaxial PMN films compared to the ferroelectric state of PMN crystals or ceramics. In the

films, the onset of the polar phase seemed to be governed by orientation of polar clusters along the direction of the applied electric field. The small threshold electric fields for the relatively fast onset of the polar phase could be ascribed to the low energy barriers between the stable states of the reorientable polar clusters in the film, compared to those in the bulk PMN. In bulk PMN, the electric field induced relaxor-to-ferroelectric transition has been found to be of percolation type, with growth and formation of new clusters.⁷ In contrast to such a transition, in PMN films, no indications of the further growth and formation of clusters were found. Rather, after the cluster reorientation (drop in permittivity) the polarization tended to saturation with its minor changes determined, perhaps, by the fluctuation mechanism.³⁵

Due to the low energy barriers of the reorientable polar clusters in the films, the “orientational” polar phase could be possibly induced by ac electric field, too [increase in H_2 in Fig. 2(b)]. Besides the orientational contribution to the dielectric permittivity, also a contribution from the motion of the walls separating the clusters was detected [evolution of δ_3 in Fig. 2(b)]. Both the orientational mechanism and the wall dynamics have been recently suggested⁴³ to determine giant permittivity and electrostriction effects in relaxors. In the present study, the mentioned mechanisms were clearly detected only under applied dc or ac electric fields, which were large enough to disturb the “pure” glass-like relaxor state. However, the possible contribution of such mechanisms to the response of the epitaxial relaxor thin films even at small fields should probably be taken into account.

The observed peculiarities of the polar phase in PMN films could be related to a specific microstructure of epitaxial films with respect to that in bulk crystals or ceramics. In epitaxial films, the presence of crystallographic strain, unavoidable presence of interfaces, possible presence of defects (misfit dislocations), and possibly peculiar B-site ordering can affect random fields, dipole moments of the clusters,

intercluster coupling, relaxation-time spectrum, etc. In particular in the studied films, a tetragonal-type distortion of the pseudocubic lattice was found (out-of-plane lattice parameter was 4.056 Å compared to that of 4.032 Å in crystal). The corresponding strain/stress could be one of the reasons for the low energy barriers between the stable states of the clusters.

An important question that remained open was connected with the crystal structure of the epitaxial PMN films in the polar state. Although neither in the present work, nor in a recent x-ray diffraction study¹³ were indications of the structural transitions detected, this could be related to the measurement technique. A more detailed x-ray diffraction analysis⁴⁴ or measurements of specific heat⁴⁵ would, probably, make it possible to reveal the transitions.

V. CONCLUSIONS

Dielectric response of epitaxial PMN thin films was experimentally studied as a function of frequency, temperature, amplitude of ac electric field, and magnitude of dc electric field. At small fields, relaxor glass-like behavior was observed. With increasing field, an onset of the polar state was detected. Compared to bulk, such an onset was characterized by the relatively low threshold fields, short critical time, and reversibility. The orientation of the polar clusters along the direction of the field and the low energy barriers between the stable states of the clusters were suggested to be responsible for the onset. The observed peculiarities could be related to the specific microstructure of the epitaxial films.

ACKNOWLEDGMENTS

The authors acknowledge the financial support of the Academy of Finland (Project No. 50941) and EU Center of Excellence CAMART, Institute of Solid State Physics, University of Latvia.

*Email address: marinat@ee.oulu.fi

¹S.-E. Park and T. R. Shroud, *J. Appl. Phys.* **82**, 1804 (1997).

²H. Arndt, F. Sauerbier, G. Schmidt, and L. Shebanov, *Ferroelectrics* **79**, 145 (1988).

³R. Sommer, N. K. Yushin, and J. J. van der Klink, *Phys. Rev. B* **48**, 13 230 (1993).

⁴E. V. Colla, E. Yu. Koroleva, N. M. Okuneva, and S. B. Vakhru-shev, *Phys. Rev. Lett.* **74**, 1681 (1995).

⁵O. Bidault, M. Licheron, E. Husson, and A. Morell, *J. Phys.: Condens. Matter* **8**, 8017 (1996).

⁶Z. G. Ye, *Ferroelectrics* **184**, 193 (1996).

⁷S. B. Vakhru-shev, J. M. Kiat, and B. Dkhil, *Solid State Commun.* **103**, 477 (1997).

⁸M. El Marssi, R. Farhi, and Yu. I. Yuzyuk, *J. Phys.: Condens. Matter* **10**, 9161 (1998).

⁹B. Dkhil and J. M. Kiat, *J. Appl. Phys.* **90**, 4676 (2001).

¹⁰Z. Kutnjak, A. Levstik, and R. Pirc, *Ferroelectrics* **270**, 283 (2002).

¹¹V. V. Gladkii, V. A. Kirikov, and E. V. Pronina, *Phys. Solid State* **45**, 1298 (2003).

¹²Z. Kighelman, D. Damjanovic, and N. Setter, *J. Appl. Phys.* **89**, 1393 (2001).

¹³N. J. Donnelly, G. Catalan, C. Morros, R. M. Bowman, and J. M. Gregg, *J. Appl. Phys.* **93**, 9924 (2003).

¹⁴M. Tyunina, V. Zauls, K. Kundzinsh, and J. Levoska, *Ferroelectrics* **270**, 241 (2002).

¹⁵M. Tyunina, V. Zauls, K. Kundzinsh, and J. Levoska, *Proc. SPIE* **5122**, 338 (2003).

¹⁶K. Kuramoto and E. Nakamura, *Ferroelectrics* **157**, 57 (1994).

¹⁷S. P. Leary and S. M. Pilgrim, *IEEE Trans. Ultrason. Ferroelectr. Freq. Control* **45**, 163 (1998).

¹⁸D. V. Taylor and D. Damjanovic, *Appl. Phys. Lett.* **73**, 2045 (1998).

¹⁹D. V. Taylor, D. Damjanovic, and N. Setter, *Ferroelectrics* **224**, 299 (1999).

²⁰R. Pirc, R. Blinc, and V. Bobnar, *Phys. Rev. B* **63**, 054203 (2001).

²¹R. Pirc, R. Blinc, and Z. Kutnjak, *Phys. Rev. B* **65**, 214101 (2002).

²²M. Tyunina, J. Levoska, A. Sternberg, and S. Leppävuori, *J. Appl. Phys.* **84**, 6800 (1998).

²³J. Levoska, M. Tyunina, A. Sternberg, and S. Leppävuori, *Ferroelectrics* **271**, 137 (2002).

²⁴M. Tyunina, J. Levoska, S. Leppävuori, and A. Sternberg, *Appl. Phys. Lett.* **78**, 527 (2001).

- ²⁵M. Tyunina and J. Levoska, Phys. Rev. B **63**, 224102 (2001).
- ²⁶C. Basceri, S. K. Streiffer, A. I. Kingon, and R. Waser, J. Appl. Phys. **82**, 2497 (1997).
- ²⁷E. V. Colla, E. Yu. Koroleva, N. M. Okuneva, and S. B. Vakhru-shev, J. Phys.: Condens. Matter **4**, 3671 (1992).
- ²⁸E. V. Colla, S. M. Gupta, and D. Viehland, J. Appl. Phys. **85**, 362 (1999).
- ²⁹M. Tyunina and J. Levoska, Ferroelectrics **291**, 93 (2003).
- ³⁰A. Levstik, Z. Kutnjak, C. Filipic, and R. Pirc, Phys. Rev. B **57**, 11 204 (1998).
- ³¹E. V. Colla, E. L. Furman, S. M. Gupta, N. Yushin, and D. Vieh-land, J. Appl. Phys. **85**, 1693 (1999).
- ³²M. Tyunina and J. Levoska, Phys. Rev. B **65**, 132101 (2002).
- ³³Z. Kutnjak, R. Pirc, and R. Blinc, Appl. Phys. Lett. **80**, 3162 (2002).
- ³⁴I. Stolichnov and A. Tagantsev, J. Appl. Phys. **84**, 3216 (1998).
- ³⁵S. A. Prosandeev, Phys. Solid State **45**, 1774 (2003).
- ³⁶C. Ang, A. S. Bhalla, and L. E. Cross, Phys. Rev. B **64**, 184104 (2001).
- ³⁷U. Bianchi, J. Dec, W. Kleemann, and J. G. Bednorz, Phys. Rev. B **51**, 8737 (1995).
- ³⁸C. Ang, L. E. Cross, R. Guo, and A. S. Bhalla, Appl. Phys. Lett. **77**, 732 (2000).
- ³⁹A. J. Bell, J. Phys.: Condens. Matter **5**, 8773 (1993).
- ⁴⁰A. E. Glazounov, A. J. Bell, and A. K. Tagantsev, J. Phys.: Con-dens. Matter **7**, 4145 (1995).
- ⁴¹L. Bellaiche and D. Vanderbilt, Phys. Rev. Lett. **83**, 1347 (1999); L. Bellaiche, J. Padilla, and D. Vanderbilt, Phys. Rev. B **59**, 1834 (1999).
- ⁴²A. K. Tagantsev and A. E. Glazounov, Phys. Rev. B **57**, 18 (1998).
- ⁴³S. A. Prosandeev, cond-mat/0207374 (2002).
- ⁴⁴J. Levoska and M. Tyunina, Ferroelectrics **291**, 11 (2003).
- ⁴⁵B. A. Strukov, S. T. Davidatze, S. N. Kravchun, S. A. Taraskin, M. Goltzman, V. V. Lemanov, and S. G. Shulman, J. Phys.: Condens. Matter **15**, 4331 (2003).